AN2520

Sensorless Field Oriented Control (FOC) for a Permanent Magnet Synchronous Motor (PMSM) Using a PLL Estimator and Equation-based Flux Weakening (FW)

INTRODUCTION

Current industry trends suggest that the Permanent Magnet Synchronous Motor (PMSM) is one of the most preferred motors by motor control application designers. Its strengths, such as high power density, fast dynamic response and high efficiency in comparison with other motors in its category, coupled with decreased manufacturing costs and improved magnetic properties, make the PMSM a good recommendation for large-scale product implementation.

Microchip Technology Inc. produces a wide range of 16-bit and 32-bit microcontrollers (MCUs) for enabling efficient, robust and versatile control of all types of motors, along with reference designs of the necessary tool sets, resulting in a fast learning curve and a shortened development cycle for new products. Refer to **"Architectural Highlights of 32-bit MCUs for Motor Control Applications"** for additional information on 32-bit MCUs for Motor Control.

FIELD ORIENTED CONTROL (FOC)

In case of the PMSM, the rotor field speed must be equal to the stator (armature) field speed (i.e., synchronous). The loss of synchronization between the rotor and stator fields causes the motor to halt.

Field Oriented Control (FOC) represents the method by which one of the fluxes (rotor, stator or air gap) is considered as a basis for creating a reference frame for one of the other fluxes with the purpose of decoupling the torque and flux-producing components of the stator current. The decoupling assures the ease of control for complex three-phase motors in the same manner as DC motors with separate excitation. This means the armature current is responsible for the torque generation, and the excitation current (for a PMSM motor, permanent magnet) is responsible for the flux generation. In this application note, the rotor flux is considered as a reference frame for the stator and air gap flux.

Several application notes from Microchip explain the principles behind FOC. Two such examples are: AN1078 *"Sensorless Field Oriented Control of PMSM Motors using dsPIC30F or dsPIC33F Digital Signal Controllers"* and AN908 *"Using the dsPIC30F for Vector Control of an ACIM"* (see **"References"**). It is beyond the scope of this application note to explain the FOC details; however, the particulars of the new implementation will be covered with respect to the previously indicated application notes.

The control scheme for FOC is presented in Figure 1. This scheme was implemented and tested using the dsPICDEM™ MCLV-2 Development Board (DM330021-2), which can drive a PMSM motor using different control techniques without requiring any additional hardware.

The control scheme is similar to the one presented in application note AN1292 *"Sensorless Field Oriented Control (FOC) for a Permanent Magnet Synchronous Motor (PMSM) Using a PLL Estimator and Field Weakening (FW)"* (see **"References"**), except for the flux weakening.

FIGURE 1: SENSORLESS FOC FOR PMSM BLOCK DIAGRAM

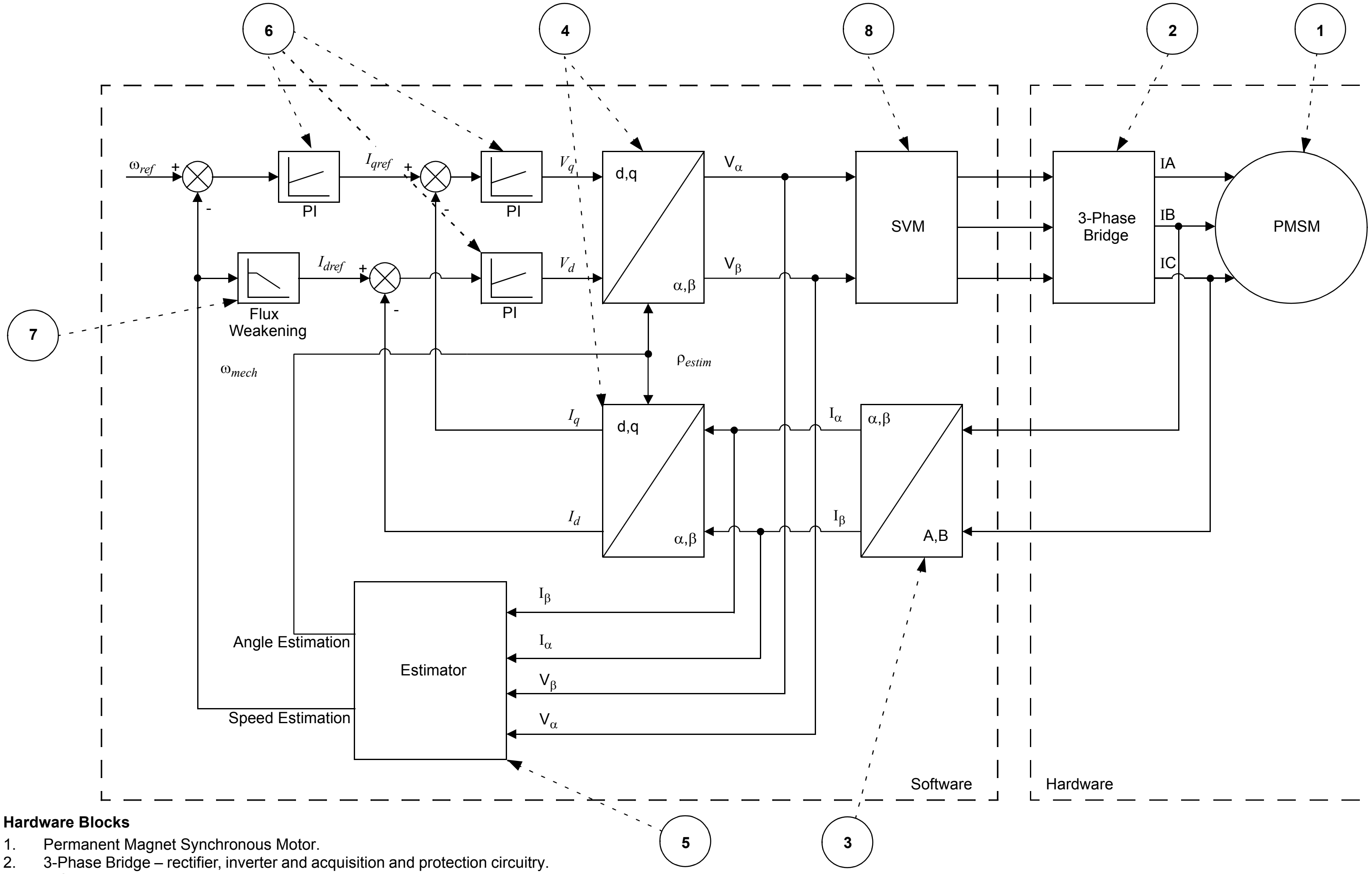

Hardware Blocks

1. Permanent Magnet Synchronous Motor.
2. 3-Phase Bridge – rectifier, inverter and acquisition and protection circuitry. software (run by the device).
3. Clarke forward transform.
4. Park forward and inverse transform.
5. Angle and speed estimator.
6. Proportional integral controller.
7. Flux weakening.
8. Space vector modulation.

The particularity of the FOC in the PMSM is that the stator's d-axis current reference I_{dref} (corresponding to the armature reaction flux on d-axis) is set to zero. The rotor's magnets produce the rotor flux linkage, Ψ_{PM}, unlike ACIM, which needs a constant reference value, I_{dref}, for the magnetizing current, thereby producing the rotor flux linkage.

The air gap flux is equal to the sum of the rotor's flux linkage, which is generated by the permanent magnets plus the armature reaction flux linkage generated by the stator current. For the constant torque mode in FOC, the d-axis air gap flux is solely equal to Ψ_{PM}, and the d-axis armature reaction flux is zero.

On the contrary, in constant power operation, the flux generating component of the stator current, I_d, is used for air gap flux weakening to achieve higher speed.

In sensorless control, where no position or speed sensors are needed, the challenge is to implement a robust speed estimator that is able to reject perturbations, such as temperature, electromagnetic noise and so on. Sensorless control is usually required when applications are cost sensitive, where moving parts are not allowed, such as position sensors or when the motor is operated in an electrically hostile environment. However, requests for precision control, especially at low speeds, should not be considered a critical matter for the given application.

The position and speed estimation is based on the mathematical model of the motor. Therefore, the closer the model is to the real hardware, the better the estimator will perform. The PMSM mathematical modeling depends on its topology, differentiating mainly two rotor types: surface-mounted and interior permanent magnet. Each type has its own advantages and disadvantages with respect to the application needs. The proposed control scheme has been developed around a surface-mounted permanent magnet synchronous motor, see Figure 2, which has the advantage of low torque ripple and lower price in comparison with other types of PMSMs. The air gap flux for the motor type considered is smooth so that the stator's inductance value, $L_d = L_q$ (non-salient PMSM), and the Back Electromotive Force (BEMF) is sinusoidal.

The fact that the air gap is large (it includes the surface mounted magnets, being placed between the stator teeth and the rotor core), implies a smaller inductance for this kind of PMSM with respect to the other types of motors with the same dimension and nominal power values. These motor characteristics enable some simplification of the mathematical model used in the speed and position estimator, while at the same time enabling the efficient use of FOC.

When using a surface PMSM, the FOC maximum torque per ampere is obtained by keeping the motor's rotor flux linkage situated at 90 degrees behind the armature generated flux linkage, see Figure 3.

FIGURE 2: SURFACE MOUNTED PM PMSM TRANSVERSAL SECTION

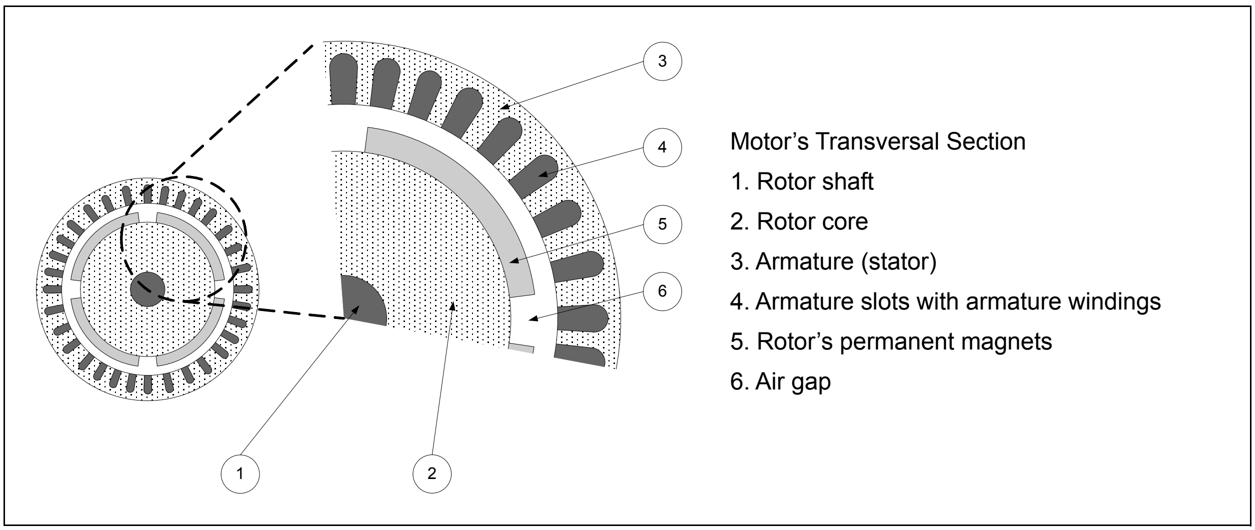

FIGURE 3: FOC PHASOR DIAGRAM (BASE SPEED)

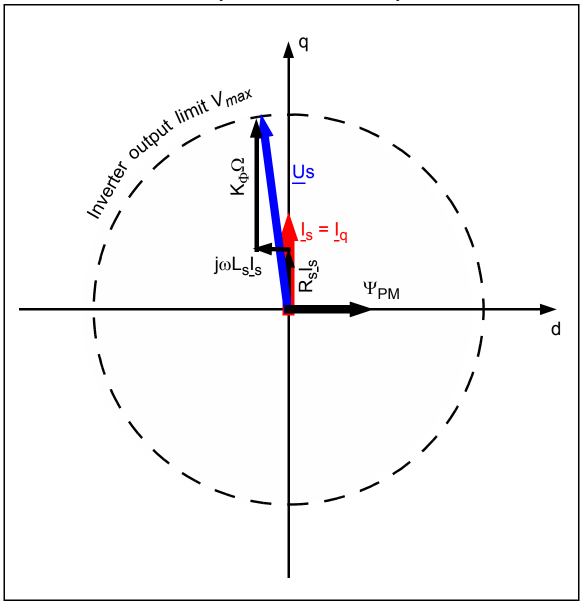

Considering the FOC constant power mode, the flux weakening for the motor considered cannot be done effectively because of the large air gap space, which implies weak armature reaction flux disturbing the rotor's permanent magnets flux linkage. Due to this, the maximum speed achieved should not exceed more than double the base speed for the motor considered for testing. Figure 4 depicts the phasors orientation in constant power, Flux Weakening (FW) mode.

FIGURE 4: FOC PHASOR DIAGRAM (HIGH-SPEED - FW)

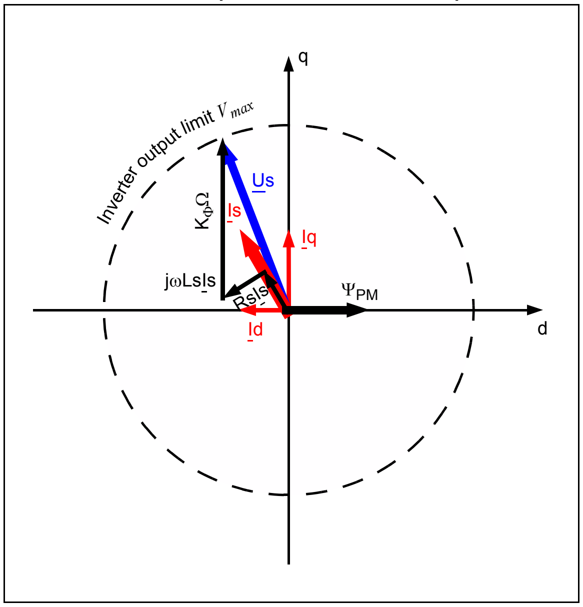

CAUTION: During flux weakening of a Surface Permanent Magnet (SPM) type of PMSM, mechanical damage of the rotor and the demagnetization of the permanent magnets is possible if careful measures are not taken or the motor manufacturer's specifications are not followed. The permanent magnets are usually bonded with an epoxy adhesive or affixed with stainless steel or carbon fiber rings. Beyond the maximum speed indicated by the manufacturer, the magnets could unbind or break, leading to destruction of the rotor, along with other mechanical parts attached to the motor's shaft. Demagnetization can be caused by exceeding the knee of flux density, B_D, for the air gap flux density, as indicated in Figure 5.

FIGURE 5: HYSTERESIS GRAPH OF PERMANENT MAGNET (THEORETICAL)

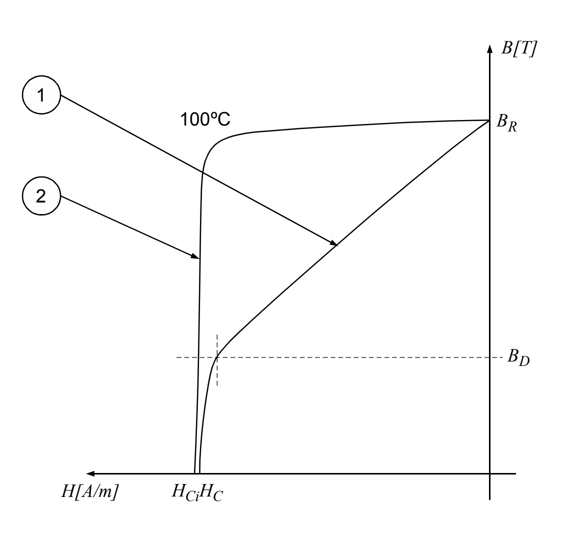

Hysteresis Graph

1. Intrinsic characteristic of permanent magnet.
2. Normal characteristic of permanent magnet.

Where:

H = Field intensity

B = Field induction

B_R = Permanent induction value

H_C = Coercivity

H_{Ci} = Intrinsic coercivity

PLL TYPE ESTIMATOR

The estimator used in this application note is an adaptation of the one presented in AN1162 *"Sensorless Field Oriented Control (FOC) of an AC Induction Motor (ACIM)"*, (see section **References**), but applied to PMSM motor particularities.

The estimator has PLL structure. Its operating principle is based on the fact that the d-component of the Back Electromotive Force (BEMF) must be equal to zero at a steady state functioning mode. The block diagram of the estimator is shown in Figure 6.

Starting from the closed loop shown in Figure 6, the estimated speed (ω_{Restim}) of the rotor is integrated to obtain the estimated angle, as shown in Equation 1:

EQUATION 1:

$$\rho_{estim} = \int \omega_{Restim} dt$$

The estimated speed, ω_{Restim}, is obtained by dividing the q-component of the BEMF value with the voltage constant, K_{Φ}, as shown in Equation 2.

EQUATION 2:

$$\omega_{Restim} = \frac{1}{K_{\Phi}}(E_{qf} - \mathrm{sgn}(E_{qf}) \cdot E_{df})$$

Considering the initial estimation premise (the d-axis value of BEMF is zero at steady state) shown in Equation 2, the BEMF q-axis value, E_{qf}, is corrected using the d-axis BEMF value, E_{df}, depending on its sign. The BEMF d-q component's values are filtered with a first order filter, after their calculation with the Park transform, as indicated in Equation 3.

EQUATION 3:

$$E_d = E_{\alpha}\cos(\rho_{estim}) + E_{\beta}\sin(\rho_{estim})$$
$$E_q = E_{\alpha}\sin(\rho_{estim}) + E_{\beta}\cos(\rho_{estim})$$

With the fixed stator frame, Equation 4 represents the stators circuit equations.

EQUATION 4:

$$E_{\alpha} = V_{\alpha} - R_S I_{\alpha} - L_S \frac{dI_{\alpha}}{dt}$$

$$E_{\beta} = V_{\beta} - R_S I_{\beta} - L_S \frac{dI_{\beta}}{dt}$$

In Equation 4, the terms containing $\alpha - \beta$ were obtained from the three-phase system's corresponding measurements through Clarke transform. L_S and R_S represent the per phase stator inductance and resistance, respectively, considering Y (star) connected stator phases. If the motor is Δ (delta) connected, the equivalent Y connection phase resistance and inductance should be calculated and used in the equations above.

Figure 7 denotes the estimator's reference electrical circuit model. The A, B and C terminals of the motor are connected to the inverter's output terminals. The voltages, V_A, V_B and V_C, represent the phase voltages applied to the motor's stator windings. V_{AB}, V_{BC} and V_{CA}, represent the line voltages between the inverter's legs, while the phase currents are I_A, I_B and I_C.

FIGURE 6: PLL ESTIMATOR'S BLOCK SCHEMATIC

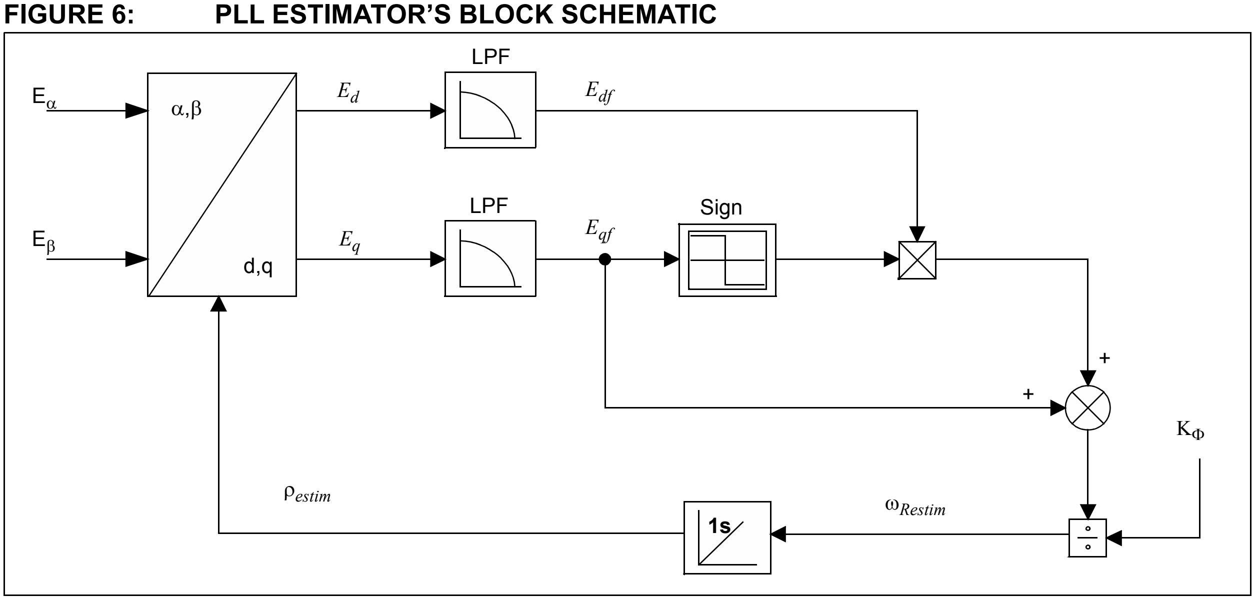

FIGURE 7: ELECTRICAL CIRCUIT MODEL FOR PLL ESTIMATOR

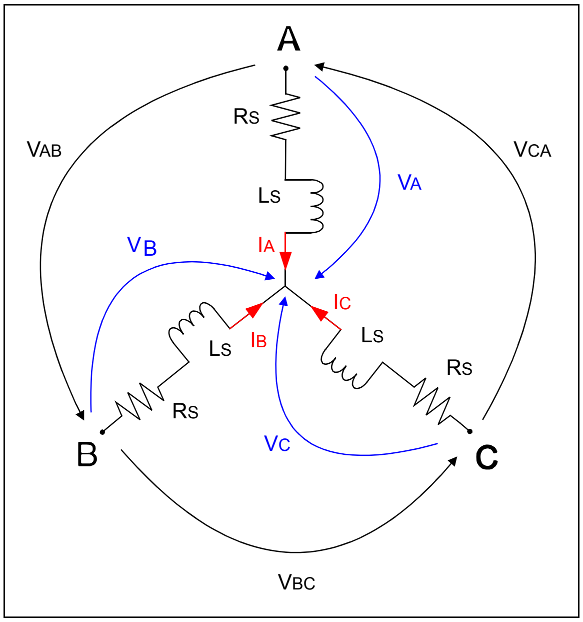

Taking one step forward concerning the equations implementation in the control system, the voltages V_α and V_β, implied in estimator's Equation 4 are a previous cycle calculation of the FOC, being fed to the Space Vector Modulation (SVM) block on the previous step of control, but also to the estimator block current step. I_α and I_β are Clarke transform results from the phase currents, which are read every estimator cycle.

The resulting E_α and E_β values of BEMF are translated to the rotating reference frame of the rotor flux through the Park transform resulting in E_d and E_q values, which conform to Equation 3. The angle ρ_{estim}, used in Park transformation is calculated on the previous execution cycle of the estimator. The d-q values of BEMF are then filtered using first order filters, entering the main condition of the estimator, based on E_d being equal to '0'.

Equation 2 reflects the calculation of ω_{Restim}, which is the resulting electrical speed. The integrated electrical speed provides the angle (ρ_{estim}) between the rotor flux and the $\alpha - \beta$ fixed stator frame. In Equation 2, K_Φ denotes the voltage constant as indicated in Table 1. The K_Φ used in the electrical speed computation, is shown in Equation 5.

EQUATION 5:

`MotorEstimParm.qInvKFi` represents:

$$\frac{1}{K_{\Phi\_Electrical}} = \sqrt{3} \cdot 2 \cdot \pi \frac{1000}{60 \cdot K_\Phi} \cdot P$$

Where:
P = Number of pole pairs and the other inputs indicated previously

The speed feedback is filtered using a first order filter identical with the one used in the BEMF case. The filter's generic form is shown in Equation 6:

EQUATION 6:

$$y(n) = y(n-1) + K_{filter} \cdot (x(n) - y(n-1))$$

Where:
$y(n)$ = Current cycle filter output
$y(n-1)$ = Previous cycle filter output
$x(n)$ = Current cycle filter input
K_{filter} = Filter constant

The DC type values at the filter's output should be free of noise from the ADC acquisition or high-frequency variations introduced by the software calculations. The filter's tuning depends on how fast the filtered values (BEMF d-q components and electrical speed) can vary, allowing for sufficient bandwidth, which reduces the possibility of useful signal loss. In the case of BEMF d-q components, two situations can be identified: (1) high speed, in the Flux Weakening mode, where their variation is slow due to the lack of sudden torque change or high acceleration ramp, and (2) low speed. The speed variation depends on the mechanical constant of the motor (and the load coupled on the motor's shaft) and the slope of the ramp-up or ramp-down limits on the speed reference, whichever is faster.

TUNING AND EXPERIMENTAL RESULTS

The algorithm tuning is very straight forward for speeds below the base speed, where the maximum torque mode is applied. Basically, the motor's parameters, measured or indicated by the manufacturer, are added to the configuration file, `mc_app.h`.

The measurement of parameters comprises the rotor's resistance, R_S, and inductance, L_S, and the voltage constant, K_Φ .

The stator resistance and inductance can be measured at the motor's terminals using a precision LCR meter. For Star connected motors: the stator phase resistance (R_S) and inductance (L_S) values are obtained by dividing the measured resistance and inductance values at the motor terminals by a factor of 2. For Delta connected motors, the stator phase resistance and inductance values are obtained by multiplying the measured resistance and inductance values at the motor terminals by a factor 1.5.

Dividing the stator phase resistance and inductance values of a Delta connected motor by a factor of 3 results in their Star connected motor equivalent phase resistance (R_S) and inductance (L_S).

This voltage constant, K_Φ, is indicated by all motor manufacturers; however, it can be measured using a very simple procedure, by rotating the rotor shaft with a constant speed, while measuring the output voltage at the motor's terminals. If the reading is done at 1000 RPM, the alternative voltage measure is a typical RMS value. Multiplying the reading value by the square root of 2 will return the value in V_{peak}/KRPM.

For the tested motor parameters, the data provided in Table 1 was measured with the procedures described above.

TABLE 1:

Motor Type	Hurst Motor DMB00224C10002	Units
Connection type	Y	—
L-L Resistance	2.1 · 2	Ohms
L-L Inductance – 1 kHz	1.92 · 2	mH
Voltage constant K_Φ	7.24	V_{peak}/ KRPM
Ambient temperature	22.7	ºC

The two necessary phase currents are read on the two shunts available on the dsPICDEM MCLV-2 Development Board and their values are scaled to the acceptable input range of the ADC module. The overall current scaling factor depends on the gain of the differential Op amp reading the shunt and the maximum value of the current passing through the motor. For example, having a phase current of 4.4A peak and a gain of 75, for a 0.005 Ohms shunt resistor, results in 3.3V present at the ADC input.

With respect to the initial calibration, the startup may be done with load, in which case the open loop ramp parameters need to be tuned.

The open loop tuning parameters include the lock time, the end acceleration speed, and the current reference value. The lock time represents the time necessary for rotor alignment, which depends on the load initial torque and moment of inertia (the larger they are, the larger the lock time value). The end speed of the initial ramp in RPM should be set sufficiently high for the estimator's calculated BEMF to have enough precision, while the time to reach that speed depends on the open loop q-axis current and resistant load attached on the motor's shaft; the larger the load, the longer the time needed for reaching the end reference speed.

The open loop is implemented as a simplification of the closed loop control, where the estimated angle between the rotor flux and the fixed reference frame is replaced by the forced angle used in open loop speed-up. The forced angle does not care about the rotor's position, but rather imposing its position, being calculated as a continuous increment fraction. An additional simplification from the control loop presented in Figure 1, is the lack of the speed controller and the current reference for the q-axis being hard-coded.

The q-axis current reference is responsible for the current forced through the motor in the open loop ramp-up; the higher the initial load, the higher the current needed, which acts as a torque reference overall.

To keep the algorithm functioning in open loop, thus disabling the closed loop transition for initial tuning purposes, enable the specific code macro definition, as shown in Example 1.

EXAMPLE 1:

```
#define OPEN_LOOP_FUNCTIONING
```

This is particularly useful for the potential PI controller's recalibration or even some initial transition conditions verifications (such as angle error between the imposed angle and the estimated one, current scaling constant experimental determination), and initial open loop ramp up parameters fine tuning, previous to the closed loop activation.

EQUATION-BASED FLUX WEAKENING

The back-EMF of the motor increases linearly with speed. Therefore, to counter the back-EMF and support the load, the applied voltage increases linearly with speed. The maximum DC bus voltage (V_{BUS}) is limited by practical considerations, such as winding insulation, motor safe operating zone, etc. In a SVPWM modulation scheme, the maximum applicable phase voltage is shown in Equation 7. For a given PMSM motor and DC bus voltage, the maximum applicable phase voltage is not sufficient to counter the generated back-EMF voltage and support the load beyond the base speed of the motor. To increase the speed of the motor beyond base speed, the generated back-EMF must be reduced, which is achieved by weakening the rotor magnetic flux, and is termed Flux Weakening mode.

EQUATION 7:

$$V_{PHASE\_MAX_{SVPWM}} = \frac{V_{BUS}}{\sqrt{3}}$$

Equation 8 shows the steady state voltage equation of the D-Q axis of the PMSM motor. The q-axis applied voltage, V_{qs} counteracts the back EMF (ω * ψ_{PM}) to drive the load at a particular speed. V_{qs} voltage is limited by maximum DC bus voltage. In order to increase the speed of the motor without increasing the DC bus voltage, the back-EMF must be reduced by lowering the rotor magnet flux linkage, ψ_{PM}. However, in a PMSM motor the flux linkage due to the rotor permanent magnets (ψ_{PM}) is constant. Thus, in PMSM motor, flux weakening is achieved by injecting negative current in d-axis (i.e., -i_{ds} such that it counteracts the rotor magnet flux linkage, ψ_{PM}).

EQUATION 8:

The dynamic d/q-axis voltage equation for the PMSM is:

$$V_d = R_s \cdot i_d - \omega \cdot L_s \cdot i_q + L_s \cdot \frac{di_d}{dt}$$

$$V_q = R_s \cdot i_q + \omega \cdot L_s \cdot i_d + \omega \cdot \Psi_{PM} + L_s \cdot \frac{di_q}{dt}$$

Since i_d and i_q are DC values, they become negligible under steady state, and therefore, the voltage equation can be rewritten as:

$$V_{ds} = R_s \cdot i_{ds} - \omega \cdot L_s \cdot i_{qs}$$

$$V_{qs} = R_s \cdot i_{qs} + \omega \cdot L_s \cdot i_{ds} + \omega \cdot \Psi_{PM}$$

Where,

V_{ds} = steady state d-axis voltage in V

V_{qs} = steady state q-axis voltage in V

i_{ds} = steady state d-axis current in A

i_{qs} = q-axis current in A

ω = Target motor electrical speed in rad/sec

L_s = Motor phase inductance in H

R_S = Motor phase resistances in Ω

During flux weakening, the negative d-axis current must be injected such that the applied voltage magnitude always lies on the voltage limit circle, V_{max}, as shown in Figure 4. Therefore, the d-axis current, i_{ds} can be calculated, as shown in Equation 9.

EQUATION 9:

$$V_{qs_{ref}} = \sqrt{V_{max}^2 - V_{ds}^2}$$

$$i_{ds_{flux\_weakening}} = \frac{V_{qs_{ref}} - R_s \cdot i_{qs} - \omega \cdot \psi_{PM}}{\omega \cdot L_s}$$

The maximum value of q-axis current is limited during flux weakening in order to ensure that the maximum magnitude of the injected current does not exceed the maximum rated motor current, as shown in Equation 10. Therefore, operation in flux weakening causes reduction in torque generating capability.

EQUATION 10:

$$lqs\_ref\,max = \sqrt{(I_{motor\_max}^2 - I_{ds\_flux\_weakening}^2)}$$

The PLL-based rotor speed estimator uses back-EMF, BEMF = ω * Kϕ, to estimate the rotor speed. While operating below the base speed, the back-EMF linearly increases with speed, and therefore, the 1/Kϕ is constant and is derived from the motor's back-EMF constant, as shown in Equation 5. However, during flux weakening, the back-EMF is maintained constant by counteracting rotor magnet flux linkage using negative d-axis current injection. Thus, maintaining constant back-EMF above the base speed would result in a variation in 1/Kϕ, which is shown in Equation 11. The variation in 1/Kϕ becomes more significant for high inductance motors or during deep field weakening (i.e., high negative d-axis current). $Ls \bullet i_{ds}$ (expressed in V-sec) is divided by 2π to match with the units of Kϕ_*Electrical* (expressed in V-sec/rad).

EQUATION 11:

$$MotorEstimParm.InvKFI\_FW = \frac{1}{K_{\phi\_Electrical} + \left(\frac{L_s \cdot i_{ds}}{2 \cdot \pi}\right)}$$

Another concern during the Flux Weakening mode is voltage limitation of the inverter. This voltage limitation is translated to the maximum achievable values for d-q current components. If both components would have followed their reference values, their resulting scalar summation value would overlap the maximum value of '1'. Therefore, the maximum current permitted for q-component of the current (the torque component of the current) will result from prioritizing the d-component of the current responsible flux weakening, which is more important due to air gap flux weakening purposes. Figure 8 presents this dynamic adjustment translated to the d-q component of the voltages (d-component of voltage prioritizing).

Because estimator performance depends drastically on the parameters of the motor, the experimental results keep this premise for the conditions of the measurements. The first dependence of rotor resistance and flux constant of the motor is the temperature. A high torque is obtained using the maximum current input, resulting in high Joule losses, resulting in an increased motor temperature. This has a negative effect on the validity of the estimator's output. Please note that it is not the intention of this application note to correct or compensate for the effect of temperature on the estimation. The compensation of parameters with temperature is possible, but it varies considerably from one motor type to another, the working conditions and functional mode. As a consequence, the test results indicated below have a premise that limits the temperature effect on the estimator's output – the time for the achieved torque is limited to one minute of continuous functioning at room temperature, see Table 2.

It may be observed that the phase current measured for the last two entries in Table 2, corresponding to the flux weakening operation, are higher than the ones immediately preceding them, in normal operation speed.

TABLE 2: EXPERIMENTAL RESULTS TESTS WITH LOAD

Reference Speed (RPM)	Achieved Speed (RPM)	Load Torque (Nm)	Phase Current (A RMS)
500	500	0.1	1.280
1000	1000	0.09	1.140
1500	1500	0.08	1.035
2000	2001	0.07	0.943
2500	2501	0.04	0.542
3000	3001	0.025	0.56
3500	3504	0.029	1.06
4000	3985	0.03	1.462

Note: The experimental test results shown were conducted on the DMB0224C10002 motor.

FIGURE 8: DYNAMIC VOLTAGE ADJUSTMENT BLOCK SCHEMATIC

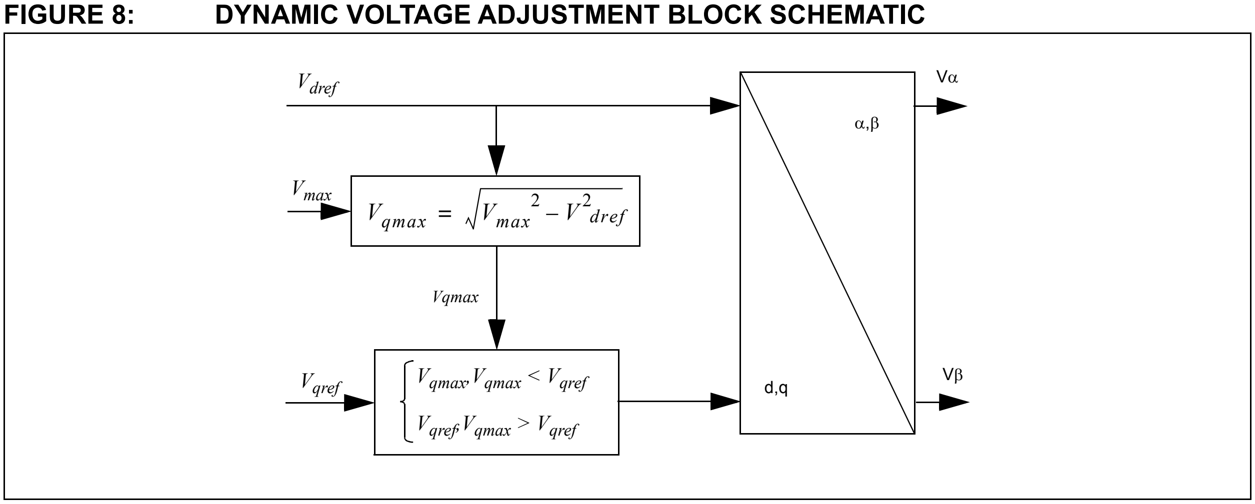

ARCHITECTURAL HIGHLIGHTS OF 32-BIT MCUS FOR MOTOR CONTROL APPLICATIONS

SAME70 Family

CPU

- 32-bit ARM® Cortex®-M7 Core - 300 MHz (2.14 DMIPS/MHz)
- DSP instruction support (2x DSP performance of Cortex-M4)
- Double-precision Floating Point Unit (FPU) - IEEE 754 Compliant
- Tightly Coupled Memory (TCM) - High-speed, Low latency, and deterministic access for time-critical code and data

ANALOG FEATURES

- Two dedicated 12-bit ADC modules with dual Sample and Hold (S&H) (i.e., capable of simultaneous sampling of four channels)
- One on-chip Analog Comparator
- Two on-chip DAC modules

PWM

- Up to eight PWM channels capable of generating complimentary PWM with dead-time in Edge/ Center-Aligned modes
- Two 2-bit gray up/down channels for stepper motor control
- Independent output override for each channel - useful for Trapezoidal control
- Two independent programmable events lines capable of generating precise and synchronized ADC triggers without any software intervention
- Asynchronous Fault inputs allow fast response PWM shutdown under Fault condition without any software intervention
- Spread Spectrum Counter - reduces acoustic noise/ electromagnetic interference of a PWM-driven motor

POSITION SENSING

On-chip Quadrature Decoder (QDEC) - input lines filtering, decoding, timer/counters to read rotor position and speed

PIC32MK Family

CPU

- 32-bit MIPS32® microAptiv™ MCU core - 120 MHz (198 DMIPS)
- DSP-enhanced core
- Double-precision Floating Point Unit (FPU) - IEEE 754 Compliant

ANALOG FEATURES

- Up to six dedicated 12-bit ADC channels plus one shared 12-bit ADC channel
- Up to four on-chip Op amp modules
- Up to five on-chip Analog Comparator modules
- Up to three on-chip DAC modules

PWM

- Up to 12 PWM pairs capable of generating complimentary PWM with dead-time in Edge-Aligned and symmetric/asymmetric Center-Aligned modes
- PWM channels capable of generating precise and synchronized ADC triggers without any software intervention
- Asynchronous Fault inputs allows fast response PWM shutdown under Fault condition without any software intervention

POSITION SENSING

On-chip QEI interfaces with incremental encoders to obtain rotor mechanical position

CONCLUSION

This application note describes a method of flux angle and speed estimation for Permanent Magnet Synchronous Motors (PMSM). This application note further describes the equation-based closed loop flux weakening.

The main theoretical ideas behind the estimator, equation-based closed loop flux weakening, and the tuning directions are also discussed. The application described in this document uses support files for the ease of adapting it to other motors. Additionally, using the indicated development hardware platform offered by Microchip for your application can significantly shorten time-to-market.

REFERENCES

"Speed Estimators, Flux Weakening and Efficient Use of SPMSM and IPMSM" - Prasad Kulkarni, 20089 MC7, Microchip MASTERs Conference 2016

The following application notes, which are referenced in this document, are available for download from the Microchip Web site (www.microchip.com):

- AN1292 *"Sensorless Field Oriented Control (FOC) for a Permanent Magnet Synchronous Motor (PMSM) Using a PLL Estimator and Field Weakening (FW)"*
- AN908 *"Using the dsPIC30F for Vector Control of an ACIM"*
- AN1078 *"Sensorless Field Oriented Control of PMSM Motors using dsPIC30F or dsPIC33F Digital Signal Controllers"*
- AN1162 *"Sensorless Field Oriented Control (FOC) of an AC Induction Motor (ACIM)"*

APPENDIX A: SOURCE CODE

All of the software covered in this application note is available as a MPLAB Harmony application. This application can be found with the `<install-dir>\apps\motor_control` folder of your MPLAB Harmony installation. The MPLAB Harmony Integrated Software framework can be downloaded from:

www.microchip.com/mplab/mplab-harmony.

APPENDIX B: REVISION HISTORY

Revision A (August 2017)

This is the initial released version of this document.

Revision B (September 2017)

This revision includes the following updates:

- The application note reference on the first page was changed to AN1292 *“Sensorless Field Oriented Control (FOC) for a Permanent Magnet Synchronous Motor (PMSM) Using a PLL Estimator and Field Weakening (FW)”*
- **TABLE 2: “EXPERIMENTAL RESULTS TESTS WITH LOAD”** was updated
- In addition, minor updates to text were implemented on page 3

NOTES:

Note the following details of the code protection feature on Microchip devices:

- Microchip products meet the specification contained in their particular Microchip Data Sheet.
- Microchip believes that its family of products is one of the most secure families of its kind on the market today, when used in the intended manner and under normal conditions.
- There are dishonest and possibly illegal methods used to breach the code protection feature. All of these methods, to our knowledge, require using the Microchip products in a manner outside the operating specifications contained in Microchip's Data Sheets. Most likely, the person doing so is engaged in theft of intellectual property.
- Microchip is willing to work with the customer who is concerned about the integrity of their code.
- Neither Microchip nor any other semiconductor manufacturer can guarantee the security of their code. Code protection does not mean that we are guaranteeing the product as "unbreakable."

Code protection is constantly evolving. We at Microchip are committed to continuously improving the code protection features of our products. Attempts to break Microchip's code protection feature may be a violation of the Digital Millennium Copyright Act. If such acts allow unauthorized access to your software or other copyrighted work, you may have a right to sue for relief under that Act.

Microchip received ISO/TS-16949:2009 certification for its worldwide headquarters, design and wafer fabrication facilities in Chandler and Tempe, Arizona; Gresham, Oregon and design centers in California and India. The Company's quality system processes and procedures are for its PIC® MCUs and dsPIC® DSCs, KEELOQ® code hopping devices, Serial EEPROMs, microperipherals, nonvolatile memory and analog products. In addition, Microchip's quality system for the design and manufacture of development systems is ISO 9001:2000 certified.

QUALITY MANAGEMENT SYSTEM CERTIFIED BY DNV

== ISO/TS 16949 ==

Trademarks

ISBN: 978-1-5224-2177-1

Worldwide Sales and Service

AMERICAS

Corporate Office
2355 West Chandler Blvd.
Chandler, AZ 85224-6199
Tel: 480-792-7200
Fax: 480-792-7277
Technical Support:
http://www.microchip.com/support
Web Address:
www.microchip.com

Atlanta
Duluth, GA
Tel: 678-957-9614
Fax: 678-957-1455

Austin, TX
Tel: 512-257-3370

Boston
Westborough, MA
Tel: 774-760-0087
Fax: 774-760-0088

Chicago
Itasca, IL
Tel: 630-285-0071
Fax: 630-285-0075

Dallas
Addison, TX
Tel: 972-818-7423
Fax: 972-818-2924

Detroit
Novi, MI
Tel: 248-848-4000

Houston, TX
Tel: 281-894-5983

Indianapolis
Noblesville, IN
Tel: 317-773-8323
Fax: 317-773-5453
Tel: 317-536-2380

Los Angeles
Mission Viejo, CA
Tel: 949-462-9523
Fax: 949-462-9608
Tel: 951-273-7800

Raleigh, NC
Tel: 919-844-7510

New York, NY
Tel: 631-435-6000

San Jose, CA
Tel: 408-735-9110
Tel: 408-436-4270

Canada - Toronto
Tel: 905-695-1980
Fax: 905-695-2078

ASIA/PACIFIC

Asia Pacific Office
Suites 3707-14, 37th Floor
Tower 6, The Gateway
Harbour City, Kowloon

Hong Kong
Tel: 852-2943-5100
Fax: 852-2401-3431

Australia - Sydney
Tel: 61-2-9868-6733
Fax: 61-2-9868-6755

China - Beijing
Tel: 86-10-8569-7000
Fax: 86-10-8528-2104

China - Chengdu
Tel: 86-28-8665-5511
Fax: 86-28-8665-7889

China - Chongqing
Tel: 86-23-8980-9588
Fax: 86-23-8980-9500

China - Dongguan
Tel: 86-769-8702-9880

China - Guangzhou
Tel: 86-20-8755-8029

China - Hangzhou
Tel: 86-571-8792-8115
Fax: 86-571-8792-8116

China - Hong Kong SAR
Tel: 852-2943-5100
Fax: 852-2401-3431

China - Nanjing
Tel: 86-25-8473-2460
Fax: 86-25-8473-2470

China - Qingdao
Tel: 86-532-8502-7355
Fax: 86-532-8502-7205

China - Shanghai
Tel: 86-21-3326-8000
Fax: 86-21-3326-8021

China - Shenyang
Tel: 86-24-2334-2829
Fax: 86-24-2334-2393

China - Shenzhen
Tel: 86-755-8864-2200
Fax: 86-755-8203-1760

China - Wuhan
Tel: 86-27-5980-5300
Fax: 86-27-5980-5118

China - Xian
Tel: 86-29-8833-7252
Fax: 86-29-8833-7256

ASIA/PACIFIC

China - Xiamen
Tel: 86-592-2388138
Fax: 86-592-2388130

China - Zhuhai
Tel: 86-756-3210040
Fax: 86-756-3210049

India - Bangalore
Tel: 91-80-3090-4444
Fax: 91-80-3090-4123

India - New Delhi
Tel: 91-11-4160-8631
Fax: 91-11-4160-8632

India - Pune
Tel: 91-20-3019-1500

Japan - Osaka
Tel: 81-6-6152-7160
Fax: 81-6-6152-9310

Japan - Tokyo
Tel: 81-3-6880- 3770
Fax: 81-3-6880-3771

Korea - Daegu
Tel: 82-53-744-4301
Fax: 82-53-744-4302

Korea - Seoul
Tel: 82-2-554-7200
Fax: 82-2-558-5932 or
82-2-558-5934

Malaysia - Kuala Lumpur
Tel: 60-3-6201-9857
Fax: 60-3-6201-9859

Malaysia - Penang
Tel: 60-4-227-8870
Fax: 60-4-227-4068

Philippines - Manila
Tel: 63-2-634-9065
Fax: 63-2-634-9069

Singapore
Tel: 65-6334-8870
Fax: 65-6334-8850

Taiwan - Hsin Chu
Tel: 886-3-5778-366
Fax: 886-3-5770-955

Taiwan - Kaohsiung
Tel: 886-7-213-7830

Taiwan - Taipei
Tel: 886-2-2508-8600
Fax: 886-2-2508-0102

Thailand - Bangkok
Tel: 66-2-694-1351
Fax: 66-2-694-1350

EUROPE

Austria - Wels
Tel: 43-7242-2244-39
Fax: 43-7242-2244-393

Denmark - Copenhagen
Tel: 45-4450-2828
Fax: 45-4485-2829

Finland - Espoo
Tel: 358-9-4520-820

France - Paris
Tel: 33-1-69-53-63-20
Fax: 33-1-69-30-90-79

France - Saint Cloud
Tel: 33-1-30-60-70-00

Germany - Garching
Tel: 49-8931-9700

Germany - Haan
Tel: 49-2129-3766400

Germany - Heilbronn
Tel: 49-7131-67-3636

Germany - Karlsruhe
Tel: 49-721-625370

Germany - Munich
Tel: 49-89-627-144-0
Fax: 49-89-627-144-44

Germany - Rosenheim
Tel: 49-8031-354-560

Israel - Ra’anana
Tel: 972-9-744-7705

Italy - Milan
Tel: 39-0331-742611
Fax: 39-0331-466781

Italy - Padova
Tel: 39-049-7625286

Netherlands - Drunen
Tel: 31-416-690399
Fax: 31-416-690340

Norway - Trondheim
Tel: 47-7289-7561

Poland - Warsaw
Tel: 48-22-3325737

Romania - Bucharest
Tel: 40-21-407-87-50

Spain - Madrid
Tel: 34-91-708-08-90
Fax: 34-91-708-08-91

Sweden - Gothenberg
Tel: 46-31-704-60-40

Sweden - Stockholm
Tel: 46-8-5090-4654

UK - Wokingham
Tel: 44-118-921-5800
Fax: 44-118-921-5820